A plant's capacity to cope with fluctuating light depends on the frequency characteristics of non-photochemical quenching and cyclic electron transport

Yuxi Niu[1], Dušan Lazár[2], Alfred R. Holzwarth[3], David M. Kramer[4],

Shizue Matsubara[1], Fabio Fiorani[1], Hendrik Poorter[1,5], Silvia D. Schrey[1], Ladislav Nedbal[1,2,6*]

[1] Institute of Bio- and Geosciences/Plant Sciences , Forschungszentrum Jülich, Wilhelm-Johnen-Straße, D-52428 Jülich, Germany

[2] Department of Biophysics, Centre of the Region Haná for Biotechnological and Agricultural Research, Faculty of Science, Palacký University, Šlechtitelů 27, 783 71 Olomouc, Czech Republic

[3] Department of Physics and Astronomy, Faculty of Science, Vrije Universiteit Amsterdam, De Boelelaan 1105, NL-1081 HV Amsterdam, The Netherlands

[4] MSU-DOE Plant Research Laboratory, Michigan State University, East Lansing, MI 48824, USA

[5] Department of Natural Sciences, Macquarie University, North Ryde, Australia

[6] PASTEUR, Department of Chemistry, École Normale Supérieure, Université PSL, Sorbonne Université, CNRS, 24, rue Lhomond, 75005, Paris, France

[*]Corresponding author: nedbal.lad@gmail.com

ORCID: 0000-0002-9627-9864 (Y.N.), 0000-0001-8035-4017 (D.L.), 0000-0002-9562-4873 (A.R.H.), 0000-0003-2181-6888 (D.M.K), 0000-0002-1440-6496 (S.M.), 0000-0001-8775-1541 (F.F.), 0000-0001-9900-2433 (H.P.), 0000-0001-5821-1968 (S.D.S.), 0000-0002-4282-3406 (L.N.)

Funding information:
Y.N., S.D.S., and L.N. gratefully acknowledge the financial support from the Federal Ministry of Education and Research of Germany (BMBF) in the framework of the YESPVNIGBEN project (03SF0576A).
D.L. and L.N. were supported by the European Regional Development Fund project "Plants as a tool for sustainable global development" (CZ.02.1.01/0.0/0.0/16_019/0000827).
D.L., S.M., and L.N. gratefully acknowledge the financial support by HORIZON-EIC-2021-PATHFINDER OPEN project DREAM (grant agreement No 101046451)
Work by DMK was supported by the U.S. Department of Energy (DOE), Office of Science, Basic Energy Sciences (BES) under Award no. DE-SC0007101.

Summary

A plant's capacity to avoid stress in fluctuating light depends on the rates at which the light changes and photoprotective regulation responds. The dynamic responses of *Arabidopsis thaliana* were probed by oscillating light inducing variations in chlorophyll fluorescence, P700, plastocyanin, and ferredoxin states as dependent on amplitudes and frequencies of the light modulation. Focusing on the roles of non-photochemical quenching (NPQ) and cyclic electron transport (CET), genotypes including the mutants *npq1*, and *npq4* for NPQ and *crr2-2*, and *pgrl1ab* for CET were involved in the study. The contrasting responses of the *npq4* mutant showed that PsbS protein played a dominant role in NPQ responding to rapid light oscillations with periods as short as 30 s. The response to slow light changes involved also the violaxanthin de-epoxidase and, possibly, thylakoid remodeling. The most dynamic segment in oscillating light of moderate amplitudes was near Photosystem I.

Keywords: cyclic electron transport, frequency domain, non-photochemical quenching, photosynthetic oscillation

Abbreviations and symbols

Parameter	**Description**
CET	Cyclic electron transport
Chl	Chlorophyll
ChlF	Chlorophyll fluorescence
$Cytb_6f$	Cytochrome b6f complex
F_0	Minimal chlorophyll fluorescence emission yield measured with the primary quinone acceptor oxidized (Q_A) in a dark-acclimated plant
F_M	Maximal chlorophyll fluorescence emission yield measured with the primary quinone acceptor reduced (Q_A^-) in a dark-acclimated plant
Fd	Ferredoxin
NIR	Near-infrared light
NPQ	Non-photochemical quenching. Multiple molecular mechanisms lead to the lowering of emission of Chl fluorescence in strong light. Here we use the term referring to mechanisms that are reversible on the scale of seconds to minutes and that involve PsbS and/or VDE proteins
NDH-like	Chloroplast NAD(P)H dehydrogenase-like complex
P700	Primary electron donor in the reaction center of photosystem I
PAR	Photosynthetically active radiation between 400 and 700 nm, measured in units $\mu mol \cdot m^{-2} \cdot s^{-1}$
PC	Plastocyanin
PSI	Photosystem I
PSII	Photosystem II
PGR5	Proton Gradient Regulation 5 protein
PGRL1	Proton Gradient Regulation-like 1 protein
PsbS	Chloroplastic 22 kDa Photosystem II protein involved in NPQ
VDE	Violaxanthin de-epoxidase enzyme
α_2 frequency domain	The domain with periods longer than 1 s and shorter than 30 s was identified by a specific dynamic behavior of ChlF in Nedbal and Lazár, 2021[1].
β_2 frequency domain	Another domain of distinct dynamics with periods longer than 1 min and shorter than 8 mint[1].

Introduction

Plants evolved in dynamic environments and oxygenic photosynthesis is resilient not only to high static irradiance but, to a large extent, also to fluctuating light[2-4]. The fluctuating excitation propagates into the photosynthetic electron transport with frequency-dependent responses determined by the reaction rates and regulation (Fig.1). Periodic filling and emptying of the biochemical pools may, without regulation, cause damage by generating transient imbalances between tightly coupled redox reactions, potentially producing noxious reactive oxygen species[5,6].

Here, we focus on the responses of non-photochemical quenching (NPQ) and cyclic electron transport (CET) that participate in plant response to fluctuating light[7-10]. The rapidly reversible component of NPQ protects the plant from transient excess light by sensing the high-light-induced acidification of the thylakoid lumen and reducing the flow of excitation energy to PSII reaction centers[11,12]. This NPQ involves protonation of the PsbS protein[8,13,14] and de-epoxidation of violaxanthin to zeaxanthin by the violaxanthin de-epoxidase enzyme (VDE)[15,16] (Fig.1B). One of the objectives of the present study is to explore if these two mechanisms act synergistically in fluctuating light or if they possibly evolved to respond at different timescales. To answer this question, we explored the dynamic response of the *npq1* mutant, which cannot convert violaxanthin into zeaxanthin by VDE[17], and the *npq4* mutant which lacks the PsbS protein[18].

CET mediates the electron transport from the reduced ferredoxin (Fd) at the acceptor side of PSI *via* $Cytb_6f$ and PC back to the donor side of PSI (Fig.1C). By the electron-coupled proton transport, CET contributes to the proton motive force for ATP synthesis, thus adjusting the ATP/NADPH ratio for downstream carbon assimilation. The CET-induced lumen acidification also contributes to NPQ, regulates electron transport and trans-thylakoid proton motive force[19], protecting both PSII and PSI[9,20-24]. *A. thaliana* plants possess two CET pathways[25]. One involves the PGR5 and PGRL1 proteins[26-29] whereas the other uses the NDH-like complex[30,31](Fig.1C), which operates also as an energy-coupled proton pump[32,33]. To discriminate between the roles played in an oscillating light by the parallel pathways of CET, we investigated the *pgrl1ab* mutant that lacks the (PGRL1/PGR5)-dependent pathway[29], and the *crr2-2* mutant impaired in the NDH-like complex-dependent pathway[34].

The methods using oscillating stimulation have been established in physics since long ago[35] and are translated to plants[36] based on a universal mathematical principle. Namely, any random, or haphazard fluctuation of light can be reproduced as a superposition of harmonic functions, each determined by the period and amplitude of a sinusoidal oscillation[37]. The essentials of the frequency analysis of photosynthetic reactions were outlined earlier[1] and its terminology is summarized in Glossary (Supplementary materials Tab.SM-1). The use of harmonically modulated light[38,39] led to identification of four frequency domains in which oxygenic photosynthesis exhibited contrasting dynamic features in a green alga[1]. Two of these domains, α_2 and β_2 that are particularly relevant in

canopies of higher plants are explored here using the model plant *A.thaliana* for which mutants with disabled mechanisms of NPQ or CET are available.

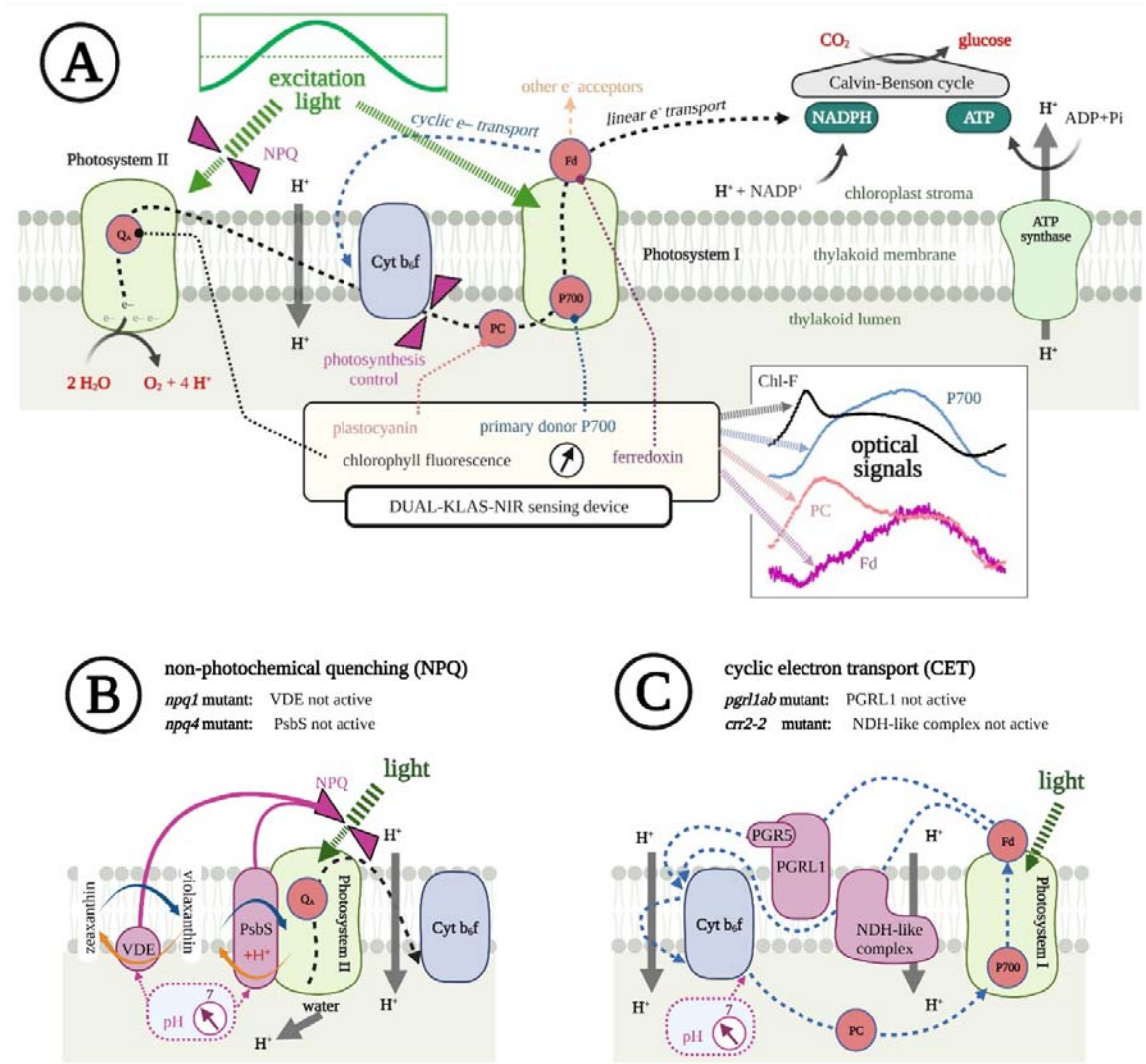

Fig.1A. A scheme of the photosynthetic apparatus in *A. thaliana* showing the linear electron transport from water to NADP+ by the black dashed line and the part of the cyclic electron transport around PSI by the blue dashed line. The components that are monitored by the measured optical proxies (bottom right) were: the Q_A redox state determining largely the Chl fluorescence yield (ChlF), plastocyanin (PC), primary donor of PSI (P700), and ferredoxin (Fd). The lumen pH-controlled regulation of the effective antenna size in PSII (NPQ) and of the electron flow from cytb_6f (photosynthesis control) are indicated by the magenta valve symbol. The harmonically modulated light is represented by one period (green line top left). The optical signals measured by the DUAL-KLAS-NIR instrument are described in Materials and Methods.

1B. The violaxanthin de-epoxidase (VDE) and PsbS protein constitute rapidly reversible non-photochemical quenching mechanisms that are reducing the excitation of PSII. Both processes are induced by low luminal pH. The cycles with blue- and orange-colored arrows represent transitions between low- and high-light states and back that occur periodically during the light oscillations.

1C. The cyclic electron transport proceeds by two parallel pathways: one *via* the Proton Gradient Regulation 5 (PGR5) and Proton Gradient Regulation-like 1 (PGRL1) complexes and the other *via* the NADH dehydrogenase-like complex (NDH-like) complex. The mutant *pgrl1ab* lacks PGRL1-PGR5-dependent pathway, whereas *crr2-2* lacks the pathway that depends on the NDH-like complex. Both CET pathways lower the luminal pH by electron-coupled proton transport. (edited based on Shikanai, 2014[25])

In all schemes, the down-pointing gray arrows represent all the processes leading to the accumulation of protons in the lumen relative to the stroma. The up-pointing gray arrow shows the dissipation of this potential difference by ATP-synthase.

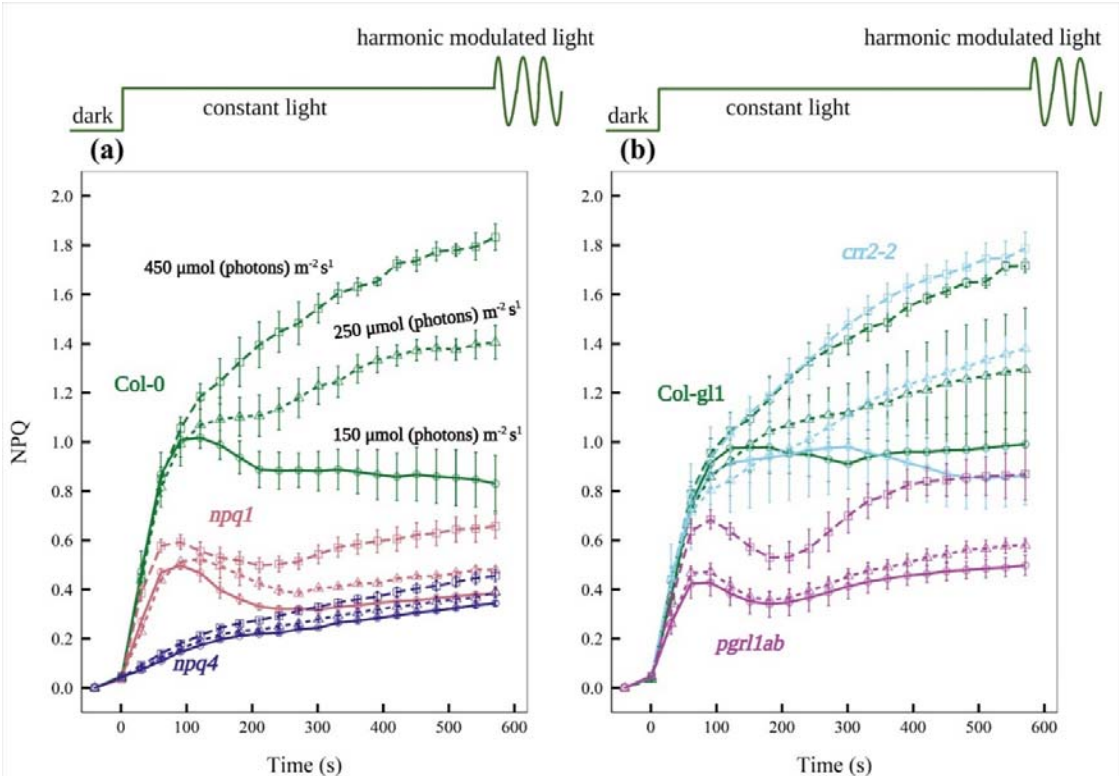

Fig.2 The dynamics of the non-photochemical quenching parameter NPQ in *A. thaliana* leaves exposed to 150 (circles), 250 (triangles), or 450 (squares) $\mu mol \cdot m^{-2} \cdot s^{-1}$ of constant PAR.
Panel (a) compares the wildtype Col-0 (green) with the mutants *npq1* (rose) and *npq4* (indigo) that are affected by knock-out of VDE and PsbS, respectively. Panel (b) compares the wild type Col-gl1 (green) with the mutants *crr2-2* (light blue) and *pgrl1ab* (magenta). The time scale marks the time of the AL exposure, with 0 s being the start of the actinic light exposure. The green-line scheme above the graphs shows that the protocol started with dark acclimation, followed by the induction in constant light, and was succeeded by the exposure to harmonically modulated light that is already connecting to the next figures. The error bars show standard errors calculated from three biological replicates**.**

Results

Induction of NPQ by constant light

The actinic effects of constant PAR were characterized by the induction kinetics of the non-photochemical quenching parameter[40] (Fig.2). The kinetics were similar in both wild types, Col-0 and Col-gl1 (Fig.2a,b), exhibiting always a fast phase, appearing tens of seconds after the light was switched on, and a slower phase developing over several minutes of illumination. The fast phase of NPQ induction in WT was largely independent of the actinic light intensity, indicating light-saturation below the lowest intensity (150 $\mu mol \cdot m^{-2} \cdot s^{-1}$). In contrast, the slower phase was light-dependent, occurring in WT in the form described earlier[41-43] only in 450 and 250 but not 150 $\mu mol \cdot m^{-2} \cdot s^{-1}$.

In the PsbS-deficient *npq4* mutant, the fast phase of the NPQ induction was nearly absent in all three tested PAR levels. In the VDE-deficient *npq1* mutant, the fast phase appeared with a reduced amplitude in form of a transient maximum at ca. 90 s. A similar transient maximum of NPQ was found in WT when the lowest light intensity (150 $\mu mol \cdot m^{-2} \cdot s^{-1}$) was used.

The *crr2-2* mutant exhibited NPQ kinetics that was qualitatively like WT[24,44]. Knocking out the NDH-like CET pathway in the mutant did not alter NPQ kinetics in the moderate PAR levels applied here. In contrast, knocking out PGR5-PGRL1 in the *pgrl1ab* mutant led to significantly altered NPQ kinetics compared to WT[45-48].

Frequency-domain analysis of photosynthetic responses to oscillating light

Eight different oscillation periods of light were sequentially applied to identify the characteristic response times of NPQ, and CET. Plants responded to the light changes by ChlF that was alternating between minima and maxima around a stationary level A_0 (Eq.1). The stationary as well as oscillatory ChlF components were dependent on the period, i.e., frequency of light oscillations in three contrasting ways that can be categorized in the α_2, and β_2 domains introduced earlier[1], and in the newly identified α_2/β_2 boundary domain (Fig.3).

The domain α_2 included the shortest periods of light oscillations. The domain was defined by ChlF response remaining in each genotype largely the same, no matter if the period was 1, 5, or 10 s.

In the boundary α_2/β_2 domain (30 or 60 s), the oscillatory ChlF component was typically higher than in the neighboring domains α_2 and β_2. This local maximum was reported earlier[38] and attributed to a resonance with a regulatory feedback. This feature, pronounced in WTs, was absent in the *npq4* mutant and was damped, probably by electron transport limitation, in the *pgrl1ab* mutant (see arguments below).

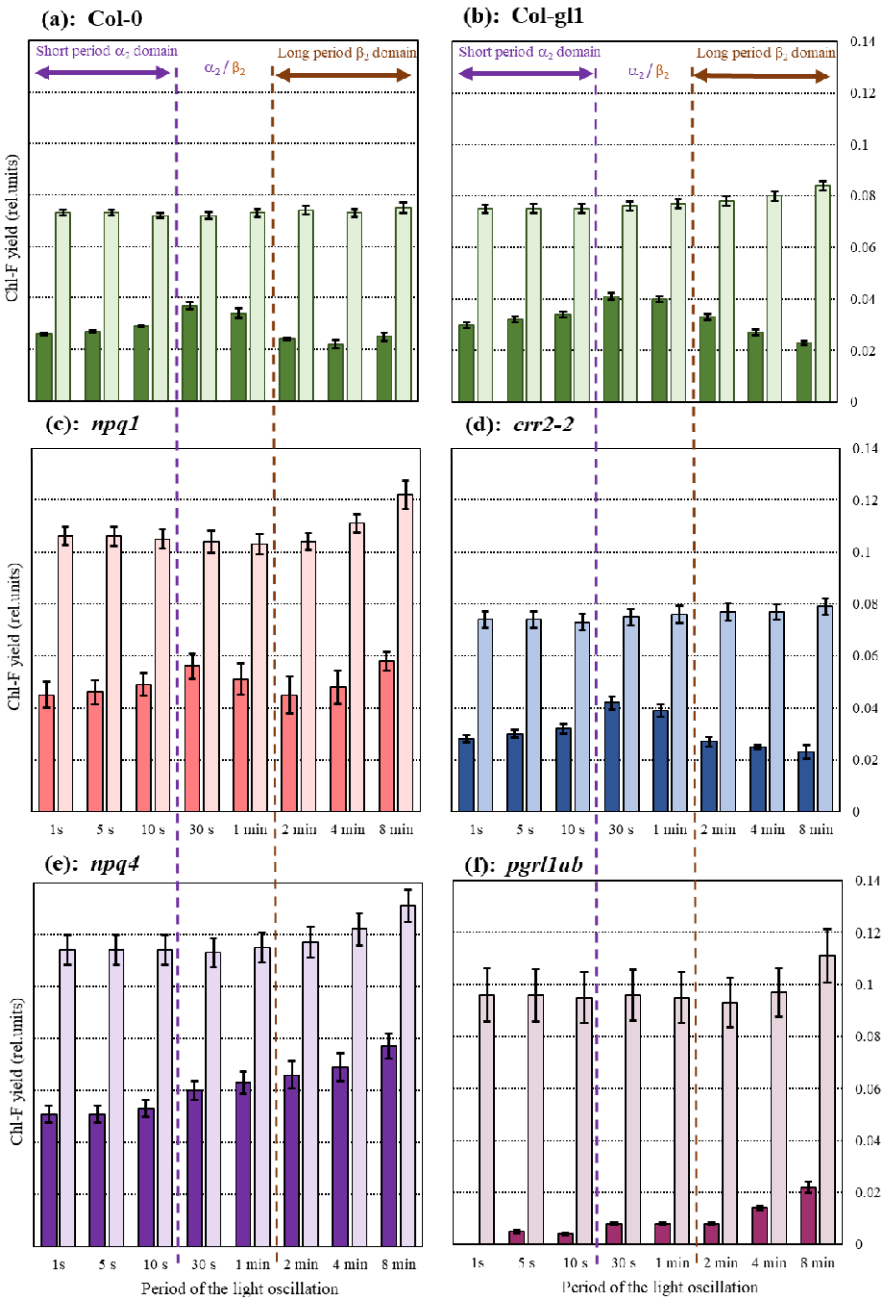

Fig.3. Stationary (light-shaded) and oscillatory (dark-shaded) components of ChlF yield measured in 6 genotypes of *A.thaliana* [panels (a)-(f)] in actinic light that was oscillating between 100 and 800 μmol·m^{-2}·s^{-1} with the short periods of 1, 5, and 10 s (α_2 domain), with periods of the 30 and 60 s (boundary α_2 / β_2 domain), and with the long periods 2, 4, ad 8 min (β_2 domain). The oscillatory component was calculated as a difference between maximum and minimum of ChlF in the light period. The error bars represent standard errors obtained from three biological replicates.

Both, the stationary and oscillatory components of the ChlF yield were increasing in the β_2 domain in the *npq1*, *npq4*, and *pgrl1ab* mutants when the period increased from 2min to 8min. This trend was absent in WTs and *crr2-2*.

Fig.3 shows by the oscillatory component only the maximum-minimum difference. The additional information including the phase shift of the extremes is presented in Fig.4A showing the entire

and period along the ordinate. The ChlF signal was mostly more complex than a simple harmonic variation, therefore, requiring for its full characterization either numerical analysis including upper harmonic components (Eq.1)[1] or presentation of entire dynamics as done here in Fig.4A.

The changes of the ChlF yield in Fig.4A were always induced by the same light pattern (top green line), oscillating between its minima of 100 $\mu mol \cdot m^{-2} \cdot s^{-1}$ at the phases 0° and 360° and maxima of 800 $\mu mol \cdot m^{-2} \cdot s^{-1}$ at the phase 180°.

Comparisons of the ChlF frequency dependence of the Col-0 WT with the *npq1* and *npq4* mutants show that both the stationary (Fig.3) as well as the variable part of ChlF (Figs.3&4A) were strongly reduced by NPQ in WT.

The most contrasting with WT was the *npq4* PsbS-deficient mutant exhibiting high amplitude ChlF variations (Fig.4A). The ChlF following closely light intensity suggests dominance of photochemical quenching with little interference of NPQ. The amplitude of the ChlF variation was monotonously increasing from shorter to longer periods. This observed dynamics of the *npq4* mutant can be explained by the PsbS protein being necessary for rapid NPQ regulation in light that oscillated with any of the periods examined in this study.

Unlike the *npq4* PsbS-deficient mutant, the *npq1* VDE-deficient mutant exhibited the ChlF yield maximum in the α_2/β_2 boundary. This difference between the *npq* mutants was visible already in Fig.3 and became obvious in Fig.4A. Corresponding ChlF maximum in the α_2/β_2 boundary was found in all biological replicates of all genotypes that were competent in the PsbS-dependent NPQ mechanism and was absent in the *npq4* PsbS-deficient mutant in all light oscillation amplitudes (Fig.4A, Fig.SM-1&2). This PsbS-dependent resonance maximum occurred with the 30 s period in both wild types at 145° phase, i.e., ca. 12 s after the light started rising from its minimum and, with the 60 s period, at 100° phase, i.e., ca. 17 s after the light minimum. The phase shift indicates that the plants and their PsbS-dependent NPQ mechanism needed 10 - 20 s to change the trend from rising to declining ChlF in the ascending light phase.

A unique response to oscillating light was found in the *pgrl1ab* mutant that was impaired in the PGR5-PGRL1 pathway (Fig.1C). The stationary part of ChlF was suppressed in *pgrl1ab* much less than in WT or in the *crr2-2* mutant (Fig.3, Fig.SM-1) while the variations around this stationary level that were caused by the light oscillations were by far smallest among all the tested genotypes (Fig.4A, Fig.SM-2). The high stationary and low oscillatory ChlF components can signal congestion of the electron transport chain on the acceptor side of PSII in the α_2 domain and α_2/β_2 boundary. Unlike in WT and in the *crr2-2* mutant, the variations of ChlF yield in the *pgrl1ab* mutant exposed to long-period light oscillations (β_2) were stronger than in the short-period oscillations (α_2) indicating that NPQ became less effective when the periods were long. The dynamic features found in the *pgrl1ab*

mutant cannot be attributed solely to changes in CET and it is likely that the mutation impaired also the linear electron transport and affected NPQ[29,49,50].

The ChlF patterns found with the *crr2-2* mutant were like WT (Fig.3 and Fig.4A), suggesting similarly to the induction in constant light (Fig.2), that the response to oscillating light was not much affected by knocking out of the NDH-like complex-dependent pathway of CET.

Figs.4B-D represent frequency responses of apparent relative oxidation/reduction of P700, PC, and Fd, respectively. The P700 oxidation was, in all genotypes except the *pgrl1ab* mutant, following closely the oscillating light, with a high oxidation around the light maximum close to 180° and with minima around 0° and 360° (Fig.4B). The amplitude of the P700 oscillations was relatively constant for periods shorter than 1 min (α_2 and α_2/β_2) but increasing with long periods from 2 to 8 min (β_2). Compared to other genotypes tested, the *pgrl1ab* mutant showed qualitatively different frequency responses, in which the P700 redox state was largely independent of the oscillating light (Fig.4B-f). This lack of variability of the P700 redox state signaled slowing or blockage of electron flow on the acceptor side of PSI in the *pgrl1ab* mutant[23]. This presumed congestion in the linear electron transport may extend back to PSII and explain also the lack of variability of ChlF that was described above.

The frequency responses of the apparent relative PC oxidation (Fig.4C) depended strongly on the oscillation periods in all genotypes. In rapidly oscillating light (α_2), PC was more oxidized in the high light phase than around the light minima. Slow light oscillations (β_2) elicited a distinct phase dependence, in which PC was increasingly oxidized only in the first phase of the rising light. This trend was changed at a later phase of the oscillation, when the PC oxidation dropped despite of light still increasing and a saddle-type depression occurred around the light maximum.

We propose that the contrast between the PC and P700 redox changes during the slow light oscillations (Figs.4B,C) might be caused by a periodic light-induced reorganization of the thylakoids that may affect differently PC and P700[51-55]. The contrast between the P700 and PC dynamics disappeared in low light (Fig.5d,g, Fig.SM-3,4) possibly because the light was not strong enough to induce the thylakoid reorganization.

The apparent relative Fd redox states (Fig.4D) were, in WT and the *npq1* and *npq4* mutants, hardly changing between the light minima and light maxima of the rapid light oscillations (α_2). In the CET mutants, particularly in the *pgrl1ab* mutant, the apparent relative Fd proxy was signaling increasing reduction on the acceptor side of PSI in the strong light relative to the light minima. An apparent Fd reduction was occurring in the *crr2-2* mutant with the periods of 30 and 60 s, i.e., in the α_2/β_2 boundary (Fig.4D-d), where the ChlF yield exhibited a resonance feature in all PsbS-competent genotypes (Fig.4A) including *crr2-2*. In the slow light oscillations (β_2), the apparent relative Fd-proxy

signaled a high oxidation on the acceptor side of PSI around the light maxima relative to light minima in all genotypes except the *pgrl1ab* mutant.

The average intensity in the oscillations applied in Fig.4 (100-800 $\mu mol \cdot m^{-2} \cdot s^{-1}$) was significantly higher than the constant light in which the plants grew before the experiment (100 $\mu mol \cdot m^{-2} \cdot s^{-1}$). This light intensity was shown in Fig.2 to lead in WT to induction of both PsbS- and VDE-dependent NPQ. Fig.5 compares the ChlF, P700, PC, and Fd dynamics in WT for all three oscillation amplitudes: 100-200, 100-400, and 100-800 $\mu mol \cdot m^{-2} \cdot s^{-1}$ while Figs.SM1-5 show the comparison of all genotypes in all amplitudes. The ChlF patterns remained qualitatively the same regardless of the amplitude of the light oscillation. Considering that also the rapid, PsbS-dependent phase of the NPQ induction was, in the tested range, nearly light independent (Fig.2), this result confirms once more the proposed central role of the PsbS-dependent NPQ in plants response to oscillating light. The dynamic patterns of P700 remained the same in all amplitudes tested, but PC and Fd redox variations in low-light oscillations (100-200 $\mu mol \cdot m^{-2} \cdot s^{-1}$) were qualitatively different from high-light oscillations (100-800 $\mu mol \cdot m^{-2} \cdot s^{-1}$) when the periods were 2 min to 8 min (β_2 domain) (Fig.5). The contrasting response of P700 and PC as Fd across different light amplitudes also supports the hypothesis that the high light can induce thylakoid reorganization[52,56-58] when the period of the modulation is 2 min or longer.

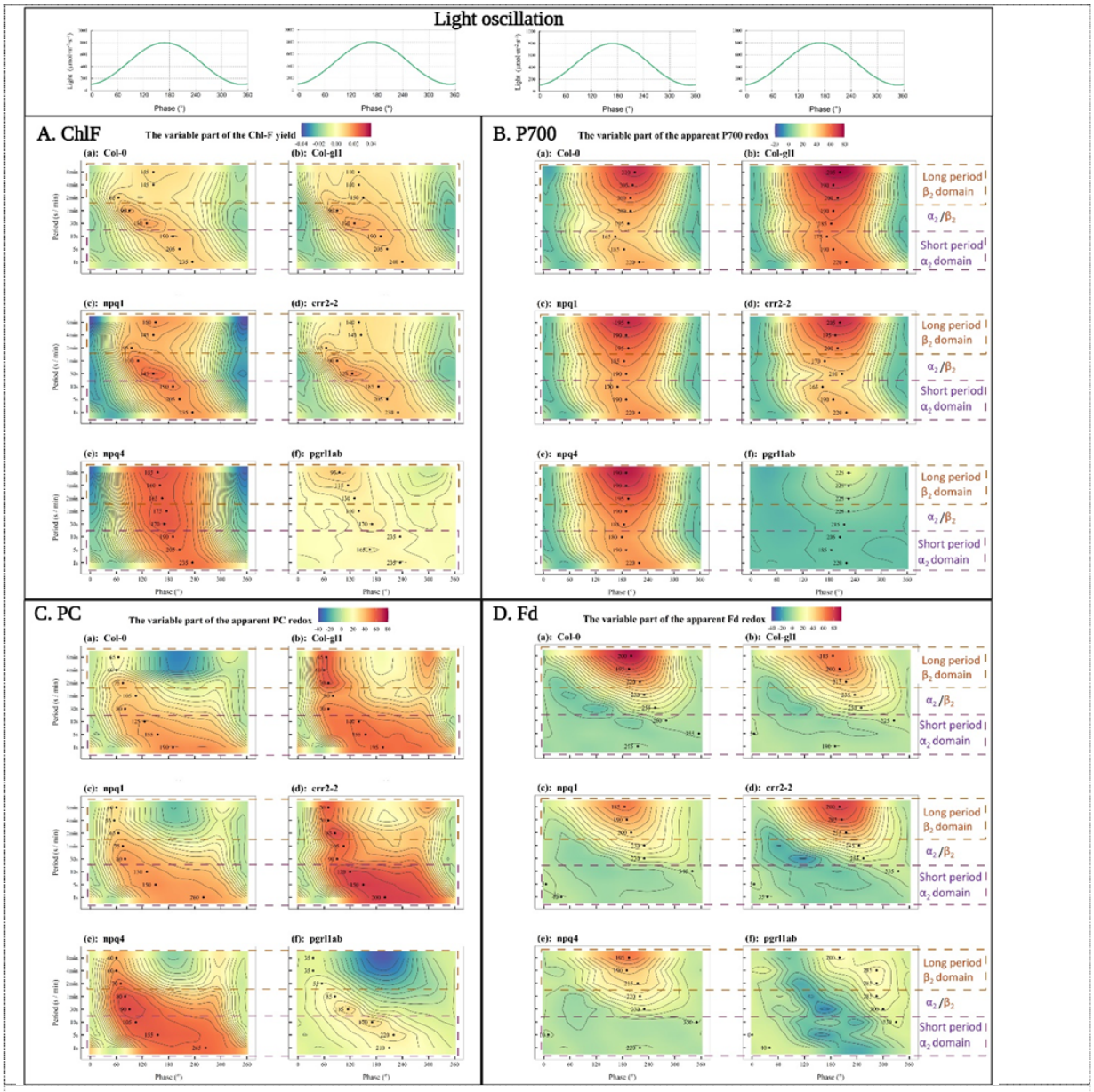

Fig.4. The time-variable part of the ChlF yield (A), P700 (B), PC (C), and Fd (D) induced in 6 genotypes of *A. thaliana* (n=3) [panels (a)-(f)] by light oscillating between 100 and 800 $\mu mol \cdot m^{-2} \cdot s^{-1}$ with the periods in the range 1 s to 8 min. The light modulation that induced the changes in the photosynthetic parameters is shown by the green line in the top row. The numbers around the signal maximum offer estimates at which phase the respective extremes of given parameter at given period occurred. The colors range from blue to red to represent the amplitude of the respective signals from low to high. The contour lines in ChlF panel (panel A) spaced at 0.025, whereas the contour lines in other panels spaced at 5. The brown dashed rectangles indicate long periods of 2, 4 and 8 min (β_2 domain), and the purple dashed rectangles indicate short periods of 1, 5, and 10 s (α_2 domain). The α_2/β_2 represents the boundary domain.

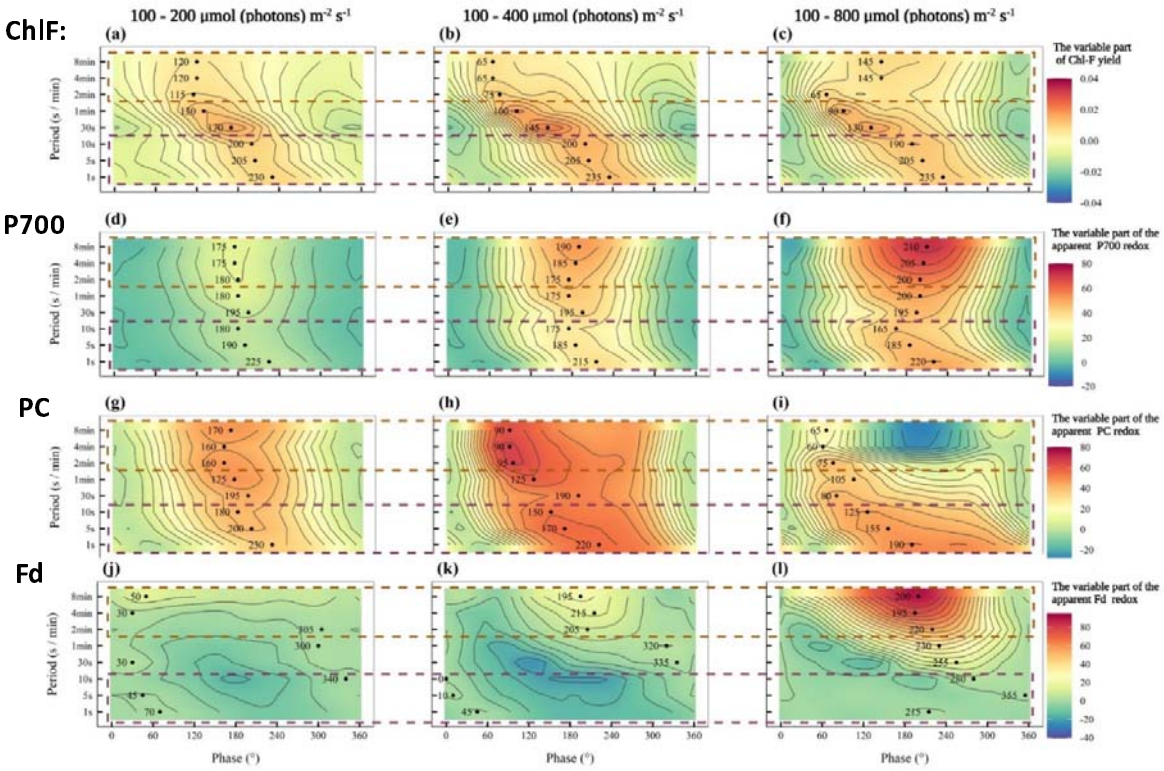

Fig.5. Comparison of the variable part of chlorophyll fluorescence yield [panels (a)-(c)] and apparent redox changes of P700 [panels (d)-(f)], PC [panels (g)-(i)] & Fd [panels (j)-(l)] in WT *A.thaliana* Col-0, under three different light oscillatory amplitudes: 100-200 $\mu mol \cdot m^{-2} \cdot s^{-1}$, 100–400 $\mu mol \cdot m^{-2} \cdot s^{-1}$, 100-800 $\mu mol \cdot m^{-2} \cdot s^{-1}$, with the periods in the range 1 s to 8 min. The numbers around the signal maxima (black dot) offer estimates at which phase the extreme occurred. The colors range from blue to red represent the change of variable part of chlorophyll fluorescence yield from low to high, with contour lines spaced at 0.025, and represent the change of variable part of P700, PC and Fd from low to high oxidation, with contour line spaced at 5. The brown dashed rectangles indicate long periods of 2, 4 and 8 min (β_2 domain), and the purple dashed rectangles indicate short periods of 1, 5, and 10 s (α_2 domain). The α_2/β_2 represents the boundary domain.

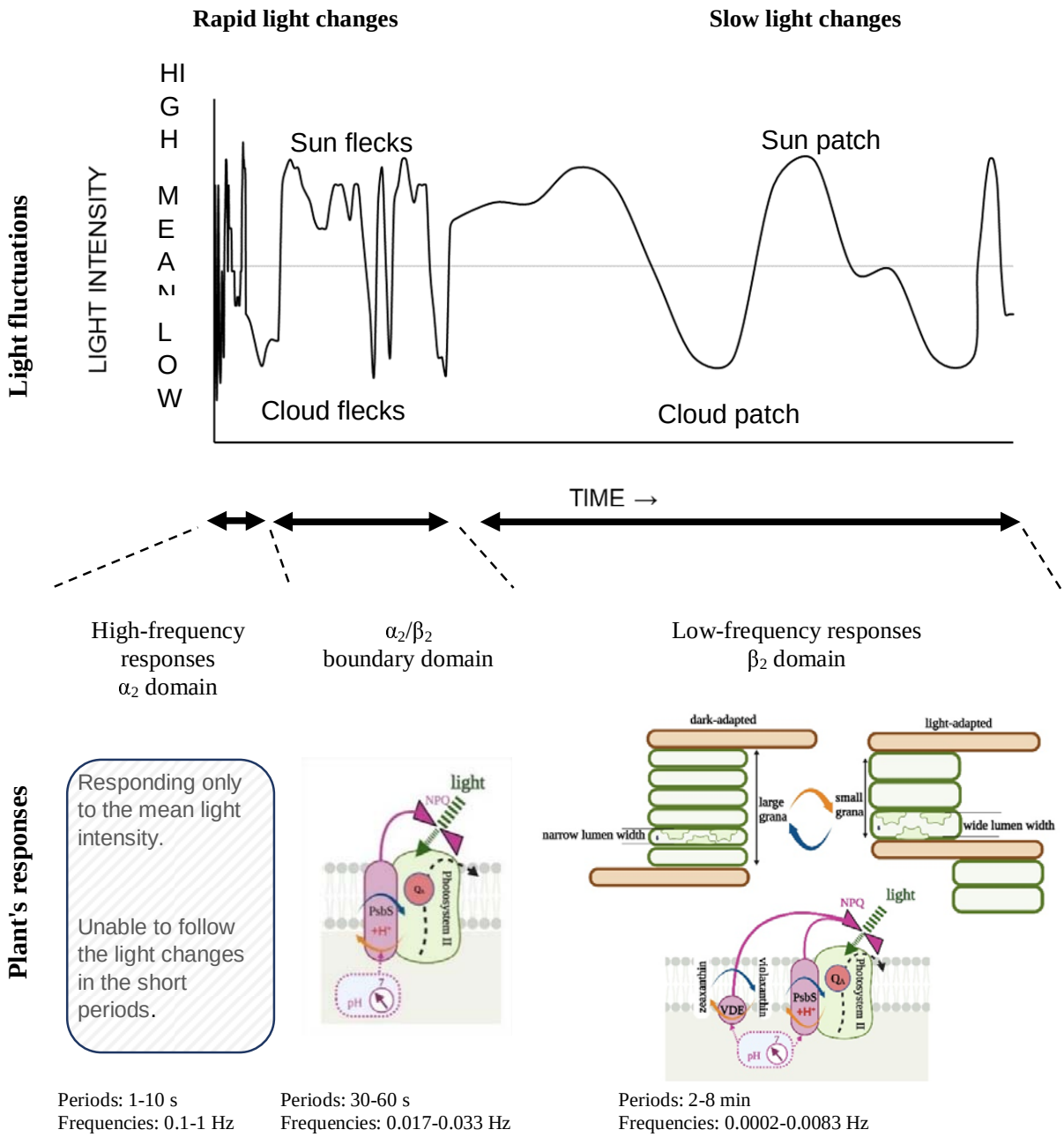

Fig.6. The top panel represents schematically natural light fluctuations occurring within plant canopies[59,60], often caused by transient gaps in the upper canopy[61], wind induced canopy movement[62] and intermittent cloudiness[63]. The elemental harmonic components contributing to the natural fluctuations are classified into three frequency domains in which distinct dynamic responses occur. The bottom row represents schematically a hypothesis that is proposed to explain observed frequency responses of WT and *npq1* and *npq4* genotypes. The NPQ response in the α_2/β_2 is proposed to be PsbS-dependent. The response to slow oscillations in the β_2-domain is, in addition formed also by VDE-dependent NPQ that is proposed to occur with periodic reorganization of the thylakoid membrane. The dark- or low-light adapted thylakoids are organized in large grana with narrow lumen space, reducing the area of contact between the grana membranes (green) and stromal lamellae (brown). With increasing the light intensity towards the maximum of the oscillation in our study, the thylakoids were proposed[53,57] to be reorganized into numerous smaller grana, creating a larger area of contact between the grana membranes (green) and stromal lamellae (brown). Thylakoid lumen volume are proposed to expand with increasing light intensity and shrink when the light was decreasing[56]. The symbols used to describe the processes in the thylakoid membrane are the same as in Fig.1.

The work identified three types of plant responses that occurred in three frequency domains of light oscillations (α_2, α_2/β_2, β_2). The results obtained with the *npq1* and *npq4* mutants led to formulating hypothesis on different dynamic limits of PsbS- dependent and VDE-dependent NPQ in natural fluctuating light (Fig.6). The contrasting responses of the *crr2-2* and *pgrl1ab* CET mutants also supported the notion that parallel pathways or mechanisms acting towards the same function respond differently to different frequencies of the fluctuating light.

The light oscillations in the α_2 domain were rapid and NPQ, being unable to follow the fast changes, responded mainly to the mean irradiance. This reduced both stationary as well as oscillatory components of ChlF. NPQ was strongest in the organisms that were competent both in the PsbS- as well as VDE-dependent quenching and weakest in the *npq4* PsbS-deficient mutant. All reporter signals in Fig.4 were following the rapid light modulation with a small delay which can be expected for unregulated system of reactant pools that are filled and emptied by photosynthetic light reactions. The delay was larger for the fastest light oscillations indicating inertia of the pools. The only exception was the *pgrl1ab* mutant in which the electron transport was presumably congested, eliminating largely any variability[23].

The boundary α_2/β_2 domain, represented by periods 30 and 60 s, was characterized by a crest maximum of ChlF that was found in plants competent in the PsbS-dependent NPQ and was absent in the *npq4* mutant missing PsbS[18]. This dynamic feature can be assigned to the onset of the PsbS-dependent NPQ in light periods as short as 30 s. We propose that with these short periods, the VDE-dependent regulation was unable to respond fast enough and the PsbS-dependent NPQ defined the plant's dynamic response in this domain alone. This may also be responsible for the resonance identified earlier[38] as well for the long-enigmatic spontaneous oscillations in plants[64,65].

The light oscillations in the β_2 domain were slow and the ChlF yield was strongly suppressed both in its stationary as well as oscillatory components by PsbS- as well as VDE-dependent NPQ. The redox changes near PSI that were induced by slowly oscillating light occurred in WT with high amplitudes despite efficient NPQ. The contrasts between the P700, PC, and Fd dynamics in the slowly oscillating light were consistent with the earlier proposals[51-55] that the thylakoid structure depends on light intensity. The slow light oscillations are thus proposed to elicit periodic changes of PsbS- and VDE-dependent NPQ together with periodically changing thylakoid organization (Fig.6). The effect of such a concerted regulation is small in the PsbS-impaired *npq4* mutant and limited in the VDE-impaired *npq1* mutant, indicating that PsbS, VDE, and thylakoid reorganization[66] are required for fully functional regulation in the slowly oscillating light.

The PsbS-dependent NPQ played in the plant's response to oscillating light in the range investigated here an indispensable role (Fig.6). The *npq4* mutant impaired in this function will, in a natural, randomly fluctuating light consisting of harmonic components from this range, experience largely

undamped oscillations in its electron transport chain and, most likely suffer from a dynamic load stress even though PAR may remain in the oscillations far below high levels that may cause photoinhibition in a static light.

Experiments using the KLAS-NIR spectrometer also revealed that the redox changes in and near PSI that were induced by oscillating light remained highly dynamic despite effective NPQ regulation in WT plants. In the slow oscillation β_2 domain, the dynamics of P700 was profoundly differed from those of PC. This may seem as contradicting the close interaction between the two redox components, with PC shuttling electrons from Cyt b_6f to P700. We propose that the PC dynamics, unlike P700 dynamics is modulated by a factor that connects both photosystems, such as photosynthesis control[21,67,68] and/or systemic properties such as changing thylakoid topology[52-55] that affects PC diffusion[56]. The remodeling of the thylakoid membrane structure in slowly oscillating light may affect pronouncedly the heterogeneity of the plastoquinone pool and Cytb_6f in granal and stromal segments of the thylakoid membranes[58,69,70]. The PQ pool in the grana thylakoid domains participates in the linear electron transport from PSII to Cyt b_6f whereas the PQ pool in the stromal thylakoid domains serves primarily for CET (see Fig.1). Further, one ought to consider that PC transports electrons from Cytb_6f to P700 over long distance[71], presumably with a low probability of backward electron transfer from P700 to PC and is subject to photosynthesis control[68]. The proposed effect of the thylakoid remodeling on the photosynthetic dynamics needs to be further examined because it may entail fundamental consequences for studies that are based on the dark-to-light transitions in the time domain. Unlike these conventional experimental protocols, the frequency-domain experiments employing oscillating light are applied to fully light-acclimated plants.

Materials and Methods

Plant Material and Growth Conditions

Arabidopsis thaliana wild type Col-0, trichome-lacking wild type Col-gl1, and the mutants affected in NPQ (*npq1, npq4*) and in CET pathways (*pgrl1ab, crr2-2*) were used in the study. Col-0 was the background of the *npq1*, *npq4*, and *pgrl1ab* mutants, and the Col-gl1 was the background of *crr2-2*. The mutant crr2-2 was kindly provided by Toshiharu Shikanai, Kyoto University, Japan and pgrl1ab by Dario Leister, Ludwig Maximilian University München, Germany. Seeds were sown in commercial soil (Pikier, Balster Einheitserdewerk, Fröndenberg, Germany). After 3 days of stratification in a 4°C dark room, the seedlings were transferred to a climate chamber with a light intensity of approx. 100 μmol m^{-2} s^{-1}, 12 h/12 h light/dark photoperiod, 26°C/20°C day/night air temperature, and 60% relative air humidity. On the 15th day after sowing, the seedlings were transferred to pots (7 × 7 × 8 cm, one plant per pot) filled with substrate (Lignostrat Dachgarten extensive, HAWITA, Vechta, Germany). The environmental conditions in the climate chamber remained the same as for the

seedlings. The plants were watered every day from the bottom to keep soil moisture throughout the cultivation and during the experiments.

Chlorophyll fluorescence and KLAS-NIR measurements

In the sixth week after sowing, chlorophyll fluorescence yield and redox changes of PC, P700, and Fd were measured simultaneously using a Dual PAM/KLAS NIR spectrophotometer with a 3010 DUAL leaf cuvette (Heinz Walz GmbH, Effeltrich, Germany). Red actinic light (630 nm) was applied to both sides of the leaf. The pulse-amplitude-modulated green light (540 nm, 6 $\mu mol \cdot m^{-2} \cdot s^{-1}$) was applied to the abaxial side of the leaf to excite chlorophyll.

In addition to chlorophyll fluorescence yield, the Dual/KLAS-NIR allows to measure four dual-wavelength difference signals of transmittance simultaneously in the near-infrared part of the spectrum using 780-820, 820-870, 870-965, and 840-965 nm wavelength pairs [72,73]. These four difference signals were deconvoluted into contributions corresponding dominantly to redox changes of ferredoxin (Fd), primary donor of PSI (P700), and plastocyanin (PC). The deconvolution relies on the selective differential transmittance spectra of P700, PC and Fd for the four wavelength pairs, which were determined by the routine called Differential Model Plots[72,73] for each genotype. The plots were always measured with 2-3 replicates. The Differential Model Plot was in this way determined for each genotype and used for the respective spectral deconvolution.

Plants were dark acclimated overnight and then remained in darkness until their dynamic properties were interrogated by the Dual PAM/KLAS NIR measurement with constant and oscillating actinic light. The measurement started with the NIR-MAX routine on a dark-acclimated plant to estimate the maximum redox changes of PC, P700, and Fd according to Klughammer & Schreiber, 2016[72]. The deconvolution of the overlapping optical transmission signals in near-infrared and the subsequent quantitative interpretation may, to some extent, be compromised by long measuring times, during which the initial deconvolution and min-max parameters may drift due to changing optical properties of the leaf. This would be of utmost importance in long conventional time-domain measurements that rely on stable reference signals, as time-domain measurements are difficult to correct for drift. With harmonically modulated light, one measures relative changes of the redox states of P700, PC, and Fd that are induced by oscillating light and the method is less sensitive to slowly drifting reference levels. The redox changes are quantified here relative to the value found at the trough of the oscillation, i.e, when the light intensity reaches its minimum. The minimum PAR was always 100 $\mu mol \cdot m^{-2} \cdot s^{-1}$. By using a reference level taken in every oscillation period, we reduced or eliminated influence of signal drift that may occur over long experimental periods. The dynamic trends occurring during the oscillations were, in this way, assessed using relative changes of the optical proxies named: apparent relative P700 and PC oxidation, and Fd reduction, respectively.

It is worth noting specific methodological aspects of the Fd signal. The implicit assumption of the NIR-MAX routine is that Fd is fully oxidized in darkness. This may not be always correct, because Fd can be reduced by multiple pathways, even in the absence of light. This potential caveat may result in an incorrect calibration of the optical proxy and in an apparent drift of the optical signal that is ascribed to fully oxidized Fd. In this situation, Fd-reduction may exceed the expected range of 0 to -100%. Therefore, we shall not base any conclusions here on the absolute numerical values of the Fd-redox state but rather focus on trends in the Fd-reduction dynamics relative to the value found at the minimum PAR (100 $\mu mol \cdot m^{-2} \cdot s^{-1}$). Further, it is worth noting that when the charge separation induced by light occurs in the PSI core complex, electron transfer from P700 to Fd occurs in a series of rapid redox reactions through A0 (the monomeric form of Chl *a*) and A1 (phylloquinone) to the [4Fe-4S] clusters (FX, FA, and FB), and ultimately to Fd [2Fe-2S][72]. In the case of *in vivo* measurements, distinguishing the absorption changes of Fd from that of the other FeS proteins is practically impossible, as the NIR differential spectrum of FA-FB is similar to that of the Fd[74], and much larger absorption changes caused by other components can influence the signal deconvolution of different FeS proteins. Therefore, the "Fd" signal used in this study is a mixture of signals of FeS components at the PSI acceptor side.

Actinic light protocols

The dynamics of photosynthesis and its regulation were studied: (1) in the time-domain by conventional induction following the dark-to-light transition; and (2) in the frequency domain using actinic light that was oscillating with periods between 1 s and 8 min.

Photosynthesis induction by constant light

Each of the dark-adapted plants was first exposed for 10 min to a constant actinic light (150, 250, or 450 $\mu mol \cdot m^{-2} \cdot s^{-1}$ / always 630 nm) to record its induction dynamics and allow acclimation to light before probing the dynamics by forced oscillations.

The saturation pulse method was applied to monitor changes in NPQ and oxidation/reduction of PC and Fd. According to this protocol, the first saturating pulse (630 nm with approx. 3700 $\mu mol \cdot m^{-2} \cdot s^{-1}$) was given in the dark to determine the maximum (F_m) chlorophyll fluorescence of PSII. After a 40-s delay, the actinic light was switched on for the next 10 min. The saturating pulses (630 nm with approx. 17000 $\mu mol \cdot m^{-2} \cdot s^{-1}$) were repeatedly triggered every 30 s. The duration of the saturating pulses was fixed at 300 ms. An example of the raw induction data is provided in *Supplementary Materials Fig.SM-6.*

Forced oscillations with changing frequencies and amplitudes

Following induction in constant actinic light, plants were exposed to light that was oscillating. The oscillations 100-200, 100-400, or 100-800 $\mu mol \cdot m^{-2} \cdot s^{-1}$ were applied to plants that were acclimated by

the previous induction in 150, 250, or 450 μmol·m^{-2}·s^{-1}, respectively. The frequency (periods) and the number of periods of sinusoidal light were set in the "Trigger Run" window in the KLAS-100 software (Heinz Walz, GmbH, Effeltrich, Germany). The periods were changing in a single continuous sequence: three periods of 8 min, five periods of each 4 min, 2 min, 1 min, 30 s, and 10 s, and finally ten periods of 5 s and 1 s. The light was controlled by an 8-bit DA-converter, yielding 256 light levels to cover the maximum range of the light intensities. The "sinusoidal" light changes were thus occurring in discrete steps rather than smoothly: The oscillations were approximated by 8 light steps for 100-200 μmol·m^{-2}·s^{-1}, 22 light steps for 100-400 μmol·m^{-2}·s^{1}, and 49 light steps for 100-800 μmol·m^{-2}·s^{-1}. The discrete character of the light changes did not affect the deconvolution into harmonic components. At least three biological replicates of each *A.thaliana* genotype were used for each treatment.

Analysis of the signals induced by oscillating light

The first period of 8 mins oscillation was largely influenced by the transition from constant to oscillating light and the first two periods of the other oscillations were influenced by the change of light frequency and, thus, were not analyzed. The later signals were already periodic and were used to extract the respective dynamic features by numeric analysis. The data representing each respective frequency in multiple replica plants were averaged to improve the signal-to-noise ratio and statistically analyzed. The signal averages were then numerically approximated by a function $Fit(t)$, consisting of a fundamental mode and of 3 upper harmonic modes as described in Nedbal & Lazár, 2021[1]:

$$Fit(t) = A_0 + A_1 \cdot \sin[\mathbf{1} \cdot \frac{2\pi(t-\tau_1)}{T}] + A_2 \cdot \sin[\mathbf{2} \cdot \frac{2\pi(t-\tau_2)}{T}] + A_3 \cdot \sin[\mathbf{3} \cdot \frac{2\pi(t-\tau_3)}{T}] + A_4 \cdot \sin[\mathbf{4} \cdot \frac{2\pi(t-\tau_4)}{T}]$$

(Eq.1)

The least-square fitting procedure was done in MS Excel and the fit yielded the offset A_0, and the amplitudes and phase shifts $\{A_1, \tau_1\}$ for the fundamental harmonics, $\{A_2, \tau_2\}$, $\{A_3, \tau_3\}$, $\{A_4, \tau_4\}$ for the upper harmonic components. Typically, no more than 2 upper harmonics were needed as adding the third upper harmonic mode did not improve χ^2 of the fit. The fitted signals of P700, PC, and Fd apparent redox changes were normalized by dividing by the signals obtained at the minimum light level (100 μmol ·m^{-2}·s^{-1}) as explained above. Each genotype is represented here by three biological replicates.

References

1 Nedbal, L. & Lazár, D. Photosynthesis dynamics and regulation sensed in the frequency domain. *Plant Physiol.* **187**, 646-661 (2021).

2 Muller, P., Li, X. P. & Niyogi, K. K. Non-photochemical quenching. A response to excess light energy. *Plant Physiol.* **125**, 1558-1566 (2001).

3 Külheim, C., Ågren, J. & Jansson, S. Rapid regulation of light harvesting and plant fitness in the field. *Science* **297**, 91-93 (2002).

4 Long, S. P. *et al.* Into the Shadows and Back into Sunlight: Photosynthesis in Fluctuating Light. *Annu. Rev. Plant. Biol.* **73**, 617-648 (2022).

5 Kono, M. & Terashima, I. Long-term and short-term responses of the photosynthetic electron transport to fluctuating light. *J. Photochem. Photobiol. B, Biol.* **137**, 89-99 (2014).

6 Kono, M., Noguchi, K. & Terashima, I. Roles of the Cyclic Electron Flow Around PSI (CEF-PSI) and O-2-Dependent Alternative Pathways in Regulation of the Photosynthetic Electron Flow in Short-Term Fluctuating Light in Arabidopsis thaliana. *Plant Cell Physiol.* **55**, 990-1004, (2014).

7 Holzwarth, A. R., Miloslavina, Y., Nilkens, M. & Jahns, P. Identification of two quenching sites active in the regulation of photosynthetic light-harvesting studied by time-resolved fluorescence. *Chem. Phys. Lett.* **483**, 262-267 (2009).

8 Ruban, A. V. Nonphotochemical Chlorophyll Fluorescence Quenching: Mechanism and Effectiveness in Protecting Plants from Photodamage. *Plant Physiol.* **170**, 1903-1916 (2016).

9 Yamamoto, H. & Shikanai, T. PGR5-Dependent Cyclic Electron Flow Protects Photosystem I under Fluctuating Light at Donor and Acceptor Sides. *Plant Physiol.* **179**, 588-600 (2019).

10 Murchie, E. H. & Ruban, A. V. Dynamic non-photochemical quenching in plants: from molecular mechanism to productivity. *Plant J.* **101**, 885-896 (2020).

11 Demmig-Adams, B., Adams, W. W., Garab, G. & Govindjee. *Non-Photochemical Quenching and Energy Dissipation in Plants, Algae and Cyanobacteria Preface*. Vol. 40 (Springer Netherlands, 2014).

12 Ware, M. A., Belgio, E. & Ruban, A. V. Comparison of the protective effectiveness of NPQ in Arabidopsis plants deficient in PsbS protein and zeaxanthin. *J. Exp. Bot.* **66**, 1259-1270 (2015).

13 Li, X. P., Müller-Moulé, P., Gilmore, A. M. & Niyogi, K. K. PsbS-dependent enhancement of feedback de-excitation protects photosystem II from photoinhibition. *Proc. Natl Acad. Sci.USA* **99**, 15222-15227 (2002).

14 Roach, T. & Krieger-Liszkay, A. The role of the PsbS protein in the protection of photosystems I and II against high light in Arabidopsis thaliana. *Biochim. Biophys. Acta - Bioenerg.* **1817**, 2158-2165 (2012).

15 Gilmore, A. M. Mechanistic aspects of xanthophyll cycle-dependent photoprotection in higher plant chloroplasts and leaves. *Physiol. Plant.* **99**, 197-209 (1997).

16 Jahns, P. & Holzwarth, A. R. The role of the xanthophyll cycle and of lutein in photoprotection of photosystem II. *Biochim. Biophys. Acta - Bioenerg.* **1817**, 182-193 (2012).

17 Niyogi, K. K., Grossman, A. R. & Björkman, O. Arabidopsis Mutants Define a Central Role for the Xanthophyll Cycle in the Regulation of Photosynthetic Energy Conversion. *Plant Cell* **10**, 1121-1134 (1998).

18 Li, X. P. *et al.* A pigment-binding protein essential for regulation of photosynthetic light harvesting. *Nature* **403**, 391-395 (2000).

19 Wang, C., Yamamoto, H. & Shikanai, T. Role of cyclic electron transport around photosystem I in regulating proton motive force. *Biochim. Biophys. Acta* **1847**, 931-938 (2015).

20 Suorsa, M. *et al.* PROTON GRADIENT REGULATION5 is essential for proper acclimation of Arabidopsis photosystem I to naturally and artificially fluctuating light conditions. *Plant Cell* **24**, 2934-2948 (2012).

21 Suorsa, M. *et al.* PGR5 ensures photosynthetic control to safeguard photosystem I under fluctuating light conditions. *Plant Signal. Behav.* **8**, e22741 (2013).

22 Yamori, W., Makino, A. & Shikanai, T. A physiological role of cyclic electron transport around photosystem I in sustaining photosynthesis under fluctuating light in rice. *Sci. Rep.* **6**, 20147 (2016).

23 Shimakawa, G. & Miyake, C. Changing frequency of fluctuating light reveals the molecular mechanism for P700 oxidation in plant leaves. *Plant Direct* **2**, e00073 (2018).

24 Nakano, H., Yamamoto, H. & Shikanai, T. Contribution of NDH-dependent cyclic electron transport around photosystem I to the generation of proton motive force in the weak mutant allele of pgr5. *Biochim. Biophys. Acta - Bioenerg.* **1860**, 369-374 (2019).

25 Shikanai, T. Central role of cyclic electron transport around photosystem I in the regulation of photosynthesis. *Curr. Opin. Biotechnol.* **26**, 25-30 (2014).

26 Munekage, Y. *et al.* PGR5 Is Involved in Cyclic Electron Flow around Photosystem I and Is Essential for Photoprotection in Arabidopsis. *Cell* **110**, 361-371 (2002).

27 Sugimoto, K. *et al.* A Single Amino Acid Alteration in PGR5 Confers Resistance to Antimycin A in Cyclic Electron Transport around PSI. *Plant Cell Physiol.* **54**, 1525-1534 (2013).

28 Hertle, A. P. *et al.* PGRL1 is the elusive ferredoxin-plastoquinone reductase in photosynthetic cyclic electron flow. *Mol. Cell* **49**, 511-523 (2013).

29 DalCorso, G. *et al.* A complex containing PGRL1 and PGR5 is involved in the switch between linear and cyclic electron flow in Arabidopsis. *Cell* **132**, 273-285 (2008).

30 Yamamoto, H., Peng, L., Fukao, Y. & Shikanai, T. An Src homology 3 domain-like fold protein forms a ferredoxin binding site for the chloroplast NADH dehydrogenase-like complex in Arabidopsis. *Plant Cell* **23**, 1480-1493 (2011).

31 Peltier, G., Aro, E. M. & Shikanai, T. NDH-1 and NDH-2 Plastoquinone Reductases in Oxygenic Photosynthesis. *Annu. Rev. Plant Biol.* 67, 55-80 (2016).

32 Strand, D. D., Fisher, N. & Kramer, D. M. The higher plant plastid NAD(P)H dehydrogenase-like complex (NDH) is a high efficiency proton pump that increases ATP production by cyclic electron flow. *J. Biol. Chem.* **292**, 11850-11860 (2017).

33 Laughlin, T. G., Savage, D. F. & Davies, K. M. Recent advances on the structure and function of NDH-1: The complex I of oxygenic photosynthesis. *Biochim. Biophys. Acta - Bioenerg.* **1861**, 148254-148254 (2020).

34 Hashimoto, M., Endo, T., Peltier, G., Tasaka, M. & Shikanai, T. A nucleus-encoded factor, CRR2, is essential for the expression of chloroplast ndhB in Arabidopsis. *Plant J.* **36**, 541-549 (2003).

35 Pintelon, R. & Schoukens, J. *System identification: a frequency domain approach*. (John Wiley & Sons, 2012).

36 Kitano, H. *Foundations of systems biology*. (The MIT Press Cambridge, Massachusetts London, England, 2001).

37 Schwartz, L. *Mathematics for the physical sciences*. (Courier Dover Publications, 2008).

38 Nedbal, L. & Březina, V. Complex Metabolic Oscillations in Plants Forced by Harmonic Irradiance. *Biophys. J.* **83**, 2180-2189 (2002).

39 Nedbal, L., Březina, V., Červený, J. & Trtílek, M. Photosynthesis in dynamic light: systems biology of unconventional chlorophyll fluorescence transients in Synechocystis sp. PCC 6803. *Photosynth. Res.* **84**, 99-106 (2005).

40 Bilger, W. & Björkman, O. Role of the xanthophyll cycle in photoprotection elucidated by measurements of light-induced absorbance changes, fluorescence and photosynthesis in leaves of Hedera canariensis. *Photosynth. Res.* **25**, 173-185 (1990).

41 Nilkens, M. *et al.* Identification of a slowly inducible zeaxanthin-dependent component of non-photochemical quenching of chlorophyll fluorescence generated under steady-state conditions in Arabidopsis. *Biochim. Biophys. Acta - Bioenerg.* **1797**, 466-475 (2010).

42 Dall'Osto, L., Cazzaniga, S., Wada, M. & Bassi, R. On the origin of a slowly reversible fluorescence decay component in the Arabidopsis npq4 mutant. *Philos. Trans. R. Soc. Lond., B, Biol. Sci.* **369**, 20130221 (2014).

43 Kress, E. & Jahns, P. The Dynamics of Energy Dissipation and Xanthophyll Conversion in Arabidopsis Indicate an Indirect Photoprotective Role of Zeaxanthin in Slowly Inducible and Relaxing Components of Non-photochemical Quenching of Excitation Energy. *Front. Plant Sci.* **8**, 2094 (2017).

44 Hashimoto, M., Endo, T., Peltier, G., Tasaka, M. & Shikanai, T. A nucleus-encoded factor, CRR2, is essential for the expression of chloroplast ndhB in Arabidopsis. *Plant J.* **36**, 541-549 (2003).

45 Munekaga, Y. *et al.* Cyclic electron flow around photosystem I is essential for photosynthesis. *Nature* **429**, 579-582 (2004).

46 Okegawa, Y., Kagawa, Y., Kobayashi, Y. & Shikanai, T. Characterization of Factors Affecting the Activity of Photosystem I Cyclic Electron Transport in Chloroplasts. *Plant Cell Physiol.* **49**, 825-834 (2008).

47 Wang, C. J., Yamamoto, H. & Shikanai, T. Role of cyclic electron transport around photosystem I in regulating proton motive force. *Biochim. Biophys. Acta - Bioenerg.* **1847**, 931-938 (2015).

48 Okegawa, Y., Basso, L., Shikanai, T. & Motohashi, K. Cyclic Electron Transport around PSI Contributes to Photosynthetic Induction with Thioredoxin f. *Plant Physiol.* **184**, 1291-1302 (2020).

49 Suorsa, M. *et al.* PGR5-PGRL1-Dependent Cyclic Electron Transport Modulates Linear Electron Transport Rate in Arabidopsis thaliana. *Mol. Plant* **9**, 271-288 (2016).

50 Wada, S., Amako, K. & Miyake, C. Identification of a Novel Mutation Exacerbated the PSI Photoinhibition in pgr5/pgrl1 Mutants; Caution for Overestimation of the Phenotypes in Arabidopsis pgr5-1 Mutant. *Cells* **10,** 2884 (2021).

51 Ruban, A. V. & Johnson, M. P. Visualizing the dynamic structure of the plant photosynthetic membrane. *Nat. Plants* **1**, 15161 (2015).

52 Ünnep, R. *et al.* Low-pH induced reversible reorganizations of chloroplast thylakoid membranes — As revealed by small-angle neutron scattering. *Biochim. Biophys. Acta - Bioenerg.* **1858**, 360-365 (2017).

53 Johnson, M. P. & Wientjes, E. The relevance of dynamic thylakoid organisation to photosynthetic regulation. *Biochim. Biophys. Acta - Bioenerg.* **1861**, 148039 (2020).

54 Li, M. *et al.* Measuring the dynamic response of the thylakoid architecture in plant leaves by electron microscopy. *Plant Direct* **4**, e00280-e00280 (2020).

55 Hepworth, C. *et al.* Dynamic thylakoid stacking and state transitions work synergistically to avoid acceptor-side limitation of photosystem I. *Nat. Plants* **7**, 87-98 (2021).

56 Kirchhoff, H. *et al.* Dynamic control of protein diffusion within the granal thylakoid lumen. *Proc. Natl Acad. Sci.USA* **108**, 20248-20253 (2011).

57 Wood, W. H. J. *et al.* Dynamic thylakoid stacking regulates the balance between linear and cyclic photosynthetic electron transfer. *Nat. Plants* **4**, 116-127 (2018).

58 Malone, L. A., Proctor, M. S., Hitchcock, A., Hunter, C. N. & Johnson, M. P. Cytochrome b6f – Orchestrator of photosynthetic electron transfer. *Biochim. Biophys. Acta - Bioenerg.* **1862**, 148380 (2021).

59 Kaiser, E., Morales, A. & Harbinson, J. Fluctuating Light Takes Crop Photosynthesis on a Rollercoaster Ride. *Plant Physiol.* **176**, 977-989 (2018).

60 Way, D. A. & Pearcy, R. W. Sunflecks in trees and forests: from photosynthetic physiology to global change biology. *Tree Physiol.* **32**, 1066-1081 (2012).

61 Chazdon, R. L. & Pearcy, R. W. The Importance of Sunflecks for Forest Understory Plants. *BioScience* **41**, 760-766 (1991).

62 Peressotti, A., Marchiol, L. & Zerbi, G. Photosynthetic photon flux density and sunfleck regime within canopies of wheat, sunflower and maize in different wind conditions. *Ital. J. Agron.* **4**, 87-92 (2001).

63 Knapp, A. K. & Smith, W. K. Stomatal and photosynthetic responses during sun/shade transitions in subalpine plants: influence on water use efficiency. *Oecologia* **74**, 62-67 (1987).

64 Delieu, T. J. & Walker, D. A. Simultaneous Measurement of Oxygen Evolution and Chlorophyll Fluorescence from Leaf Pieces. *Plant Physiol.* **73**, 534-541 (1983).

65 Lazár, D., Kaňa, R., Klinkovský, T. & Nauš, J. Experimental and theoretical study on high temperature induced changes in chlorophyll a fluorescence oscillations in barley leaves upon 2 % CO 2. *Photosynthetica* **43**, 13-27 (2005).

66 Horton, P. & Ruban, A. Molecular design of the photosystem II light-harvesting antenna: photosynthesis and photoprotection. *J. Exp. Bot.* **56**, 365-373 (2005).

67 Colombo, M. et al. Photosynthesis Control: An underrated short-term regulatory mechanism essential for plant viability. *Plant Signal. Behav.* 11, e1165382 (2016).

68 Johnson, J. E. & Berry, J. A. The role of Cytochrome b(6)f in the control of steady-state photosynthesis: a conceptual and quantitative model. *Photosynth. Res.* **148**, 101-136 (2021).

69 Joliot, P., Lavergne, J. & Béal, D. Plastoquinone compartmentation in chloroplasts. I. Evidence for domains with different rates of photo-reduction. *Biochim. Biophys. Acta - Bioenerg.* **1101**, 1-12 (1992).

70 Kirchhoff, H., Horstmann, S. & Weis, E. Control of the photosynthetic electron transport by PQ diffusion microdomains in thylakoids of higher plants. *Biochim. Biophys. Acta - Bioenerg.* **1459**, 148-168 (2000).

71 Höhner, R. *et al.* Plastocyanin is the long-range electron carrier between photosystem II and photosystem I in plants. *Proc. Natl Acad. Sci.USA* **117**, 15354-15362 (2020).

72 Klughammer, C. & Schreiber, U. Deconvolution of ferredoxin, plastocyanin, and P700 transmittance changes in intact leaves with a new type of kinetic LED array spectrophotometer. *Photosynth. Res.* **128**, 195-214 (2016).

73 Schreiber, U. & Klughammer, C. Analysis of Photosystem I Donor and Acceptor Sides with a New Type of Online-Deconvoluting Kinetic LED-Array Spectrophotometer. *Plant Cell Physiol.* **57**, 1454-1467 (2016).

74 Sétif, P., Boussac, A. & Krieger-Liszkay, A. Near-infrared in vitro measurements of photosystem I cofactors and electron-transfer partners with a recently developed spectrophotometer. *Photosynth. Res.* **142**, 307-319 (2019).

SUPPLEMENTARY MATERIALS

A plant's capacity to cope with fluctuating light depends on the frequency characteristics of non-photochemical quenching and cyclic electron transport

Yuxi Niu[1], Dušan Lazár[2], Alfred R. Holzwarth[3], David M. Kramer[4],

Shizue Matsubara[1], Fabio Fiorani[1], Hendrik Poorter[1,5], Silvia D. Schrey[1], Ladislav Nedbal[1,2,6*]

Tab.SM-1: Glossary	
amplitude	the maximum deviation from a mean; in the case of harmonically modulated light, it is one half of the difference between the light intensity maximum and minimum
angular frequency ω	the parameter of light modulation or of plant response that defines how many times a full cycle (360° in angle degrees or 2π in radian units) is completed in a unit of time. It is related to the period T as: $\omega = \frac{2\pi}{T}$
fluctuating light	randomly changing light: its intensity pattern thus cannot be predicted
forced oscillation	a repeating variation pattern of plant photosynthesis that is sustained in time by a *periodic* energy supply, here *harmonically modulated light*
frequency-domain measurement	the measurement of plant activity applying *harmonically modulated light* with *period/frequency* of the light modulation changing over a wide range; plant response(s) are measured as a function of the light modulation *frequency*
harmonically modulated light	the light intensity that consists of a variable part that is changing as a harmonic function $$a * \sin\left(\frac{2\pi}{T} \cdot t\right) + b * \cos\left(\frac{2\pi}{T} \cdot t\right)$$, where t stands for time, T is the *period*, $\frac{2\pi}{T}$ the *angular frequency* of the light variation, and a, b are parameters that define together the *amplitude* and *phase* of the light modulation.
oscillation	a repeating variation pattern of light or plant activity
period T	the time after which a process is repeated, here it applies both to the light modulation as well as to plant response elicited by the modulated excitation light
periodic	Repeating
oscillation phase	the parameter defining the progress of a periodic process: e.g., phase 0 is the origin, the phase $\frac{1}{4} \cdot 2\pi$ represents one-quarter of the full cycle, phase 2π represents the full cycle
resonance	a phenomenon of the increased *amplitude* of a measured response that occurs when the *frequency* of external forcing agrees with an internal characteristic *frequency* of the examined plant (sometimes called eigen-frequency)
spontaneous oscillation	the *oscillation* of plant activities that sometimes appear in response to an abrupt change of external conditions; spontaneous oscillations of plants are fading over time
time-domain measurement	the meaning common in fluorometry or spectroscopy of plants: the plant response to an aperiodic light change; mostly a stepwise dark-to-light or light-to-dark transition, often also the response to a short light flash measured as a function of time

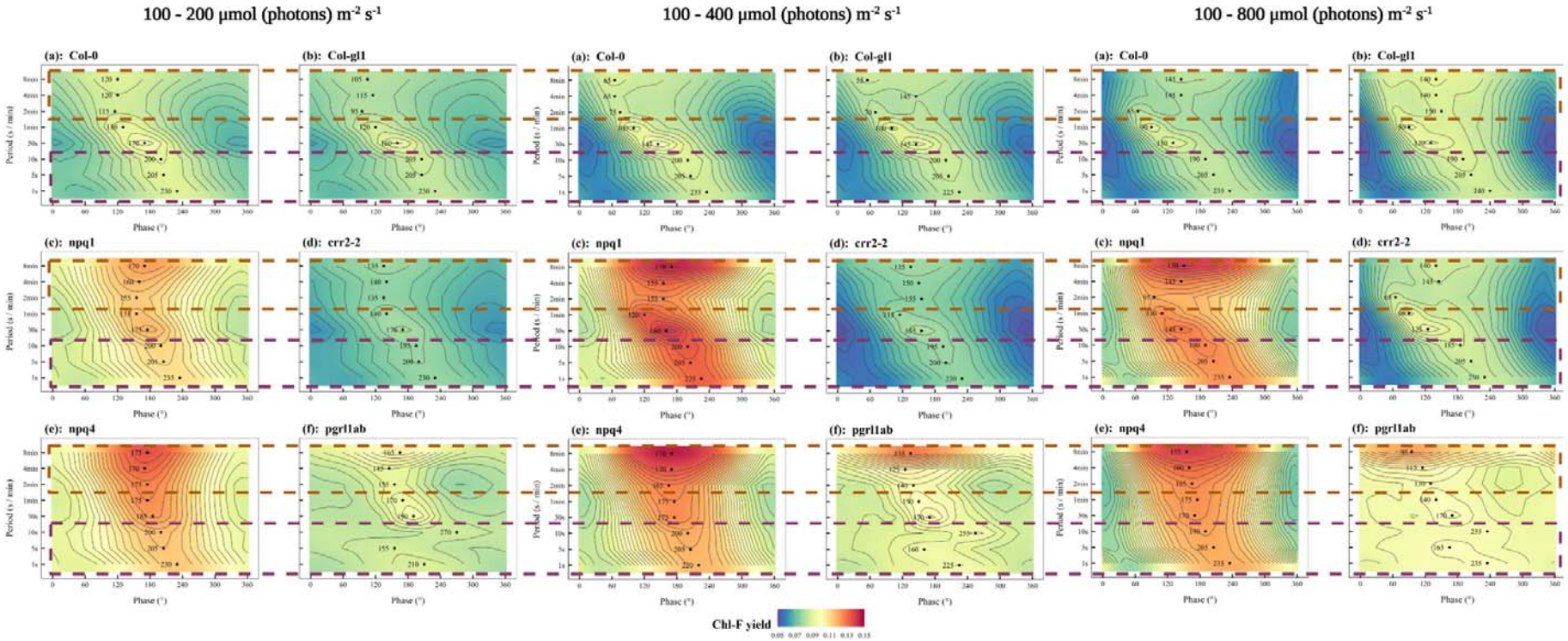

Fig.SM-1. Dynamics of chlorophyll fluorescence yield (ChlF) induced in 6 genotypes of *A. thaliana* by oscillating light with the periods in the range from 1 s to 8 min. Unlike Figs.4A in the main text and Fig.SM-2, the data here show the signal as measured, not only the oscillatory component of ChlF. Further, this figure shows data for three amplitudes of the light oscillations: The left two columns represent oscillations between 100 - 200 $\mu mol \cdot m^{-2} \cdot s^{-1}$, the middle two columns 100 - 400 $\mu mol \cdot m^{-2} \cdot s^{-1}$, and the right two columns 100 - 800 $\mu mol \cdot m^{-2} \cdot s^{-1}$. The numbers around the black points inside the graphs offer estimates at which phase particular maximum occurred. The colors range from blue to red to represent the change of chlorophyll fluorescence yield from low to high, with contour lines spaced at 0.025. The brown dashed rectangles indicate long periods of 2, 4 and 8 min (β_2 domain), and the purple dashed rectangles indicate short periods of 1, 5, and 10 s (α_2 domain).

The variable part of chlorophyll fluorescence yield in oscillating light

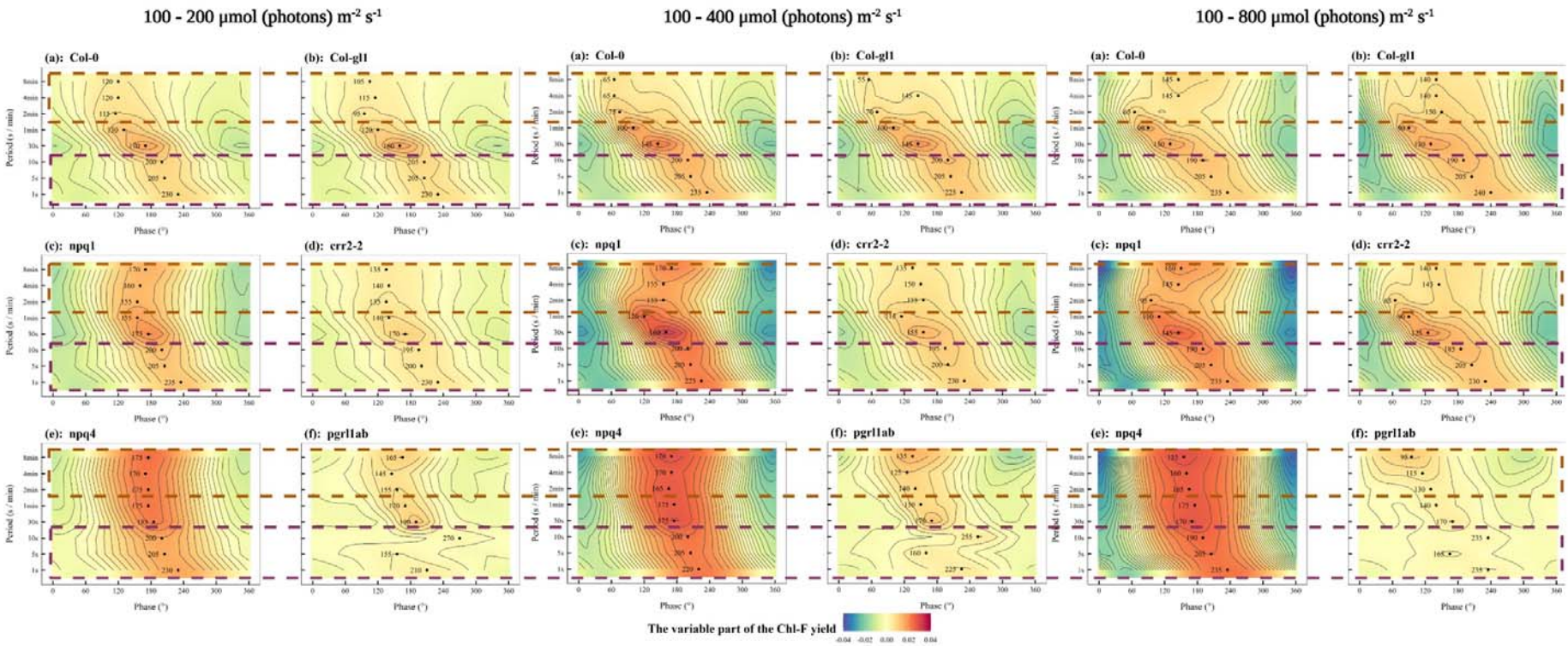

Fig.SM-2. The same ChlF data as in Fig.SM-1 after subtracting the stationary ChlF component. In this format, some dynamic features are more visible than in Fig.SM-1.

The variable part of the apparent relative P700 oxidation

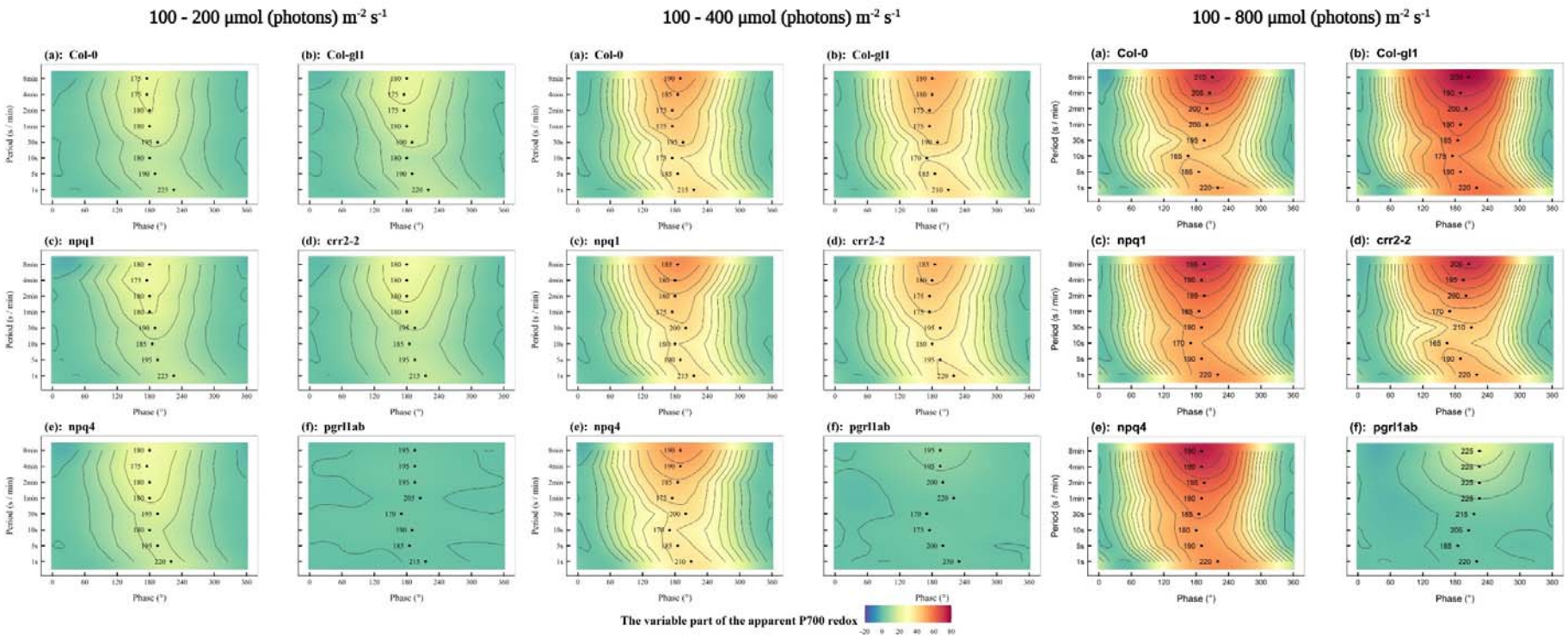

Fig.SM-3. The variable part of apparent relative P700 oxidation induced in 6 genotypes of *A. thaliana* (n=3) by three different amplitudes of oscillating light. The structure of the graph and the legends are the same as in Fig.SM-1, only the color scale from blue to red to represents the apparent change of P700 redox state from low to high, with contour lines spaced at 5.

The variable part of the apparent relative PC oxidation

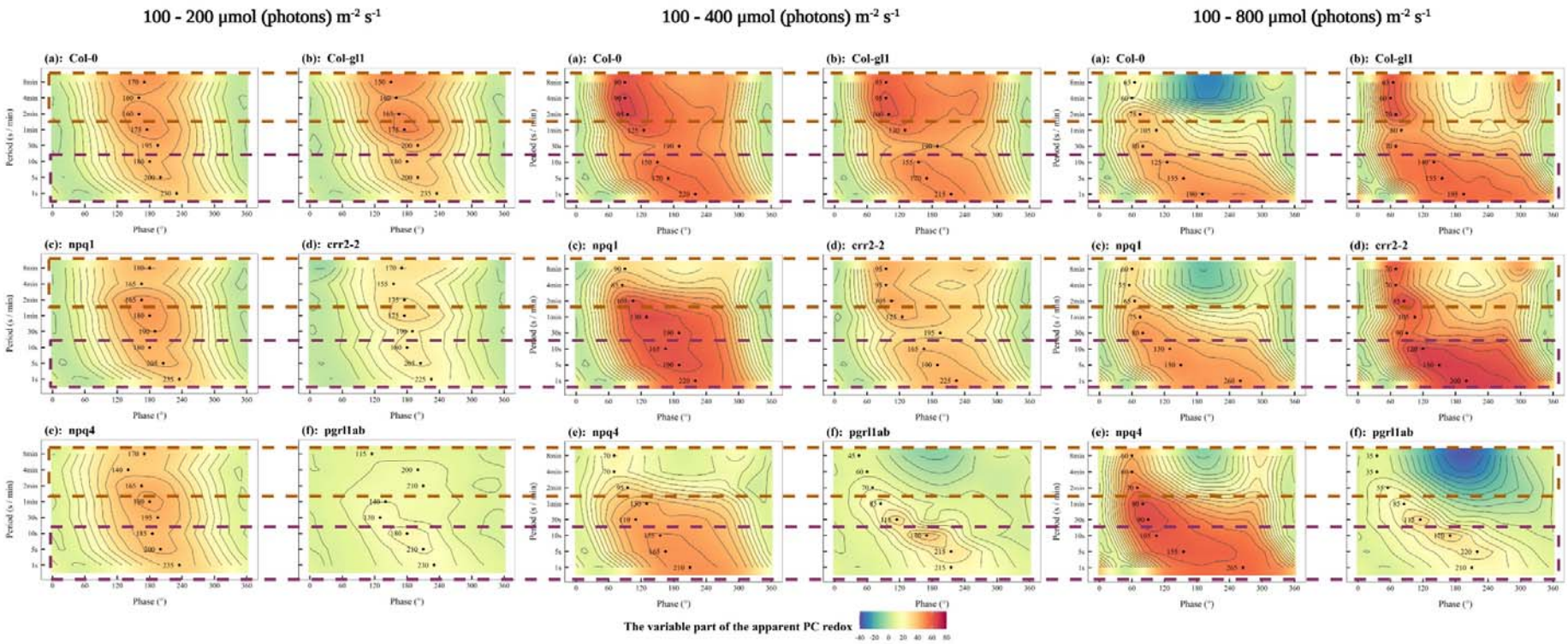

Fig.SM-4. The variable part of apparent relative PC oxidation induced in 6 genotypes of *A. thaliana* (n=3) by three different amplitudes of oscillating light. The structure of the graph and the legends are the same as in Fig.SM-1, only the color scale from blue to red to represents the apparent change of PC oxidation from low to high, with contour lines spaced at 5.

The variable part of the apparent relative Fd oxidation

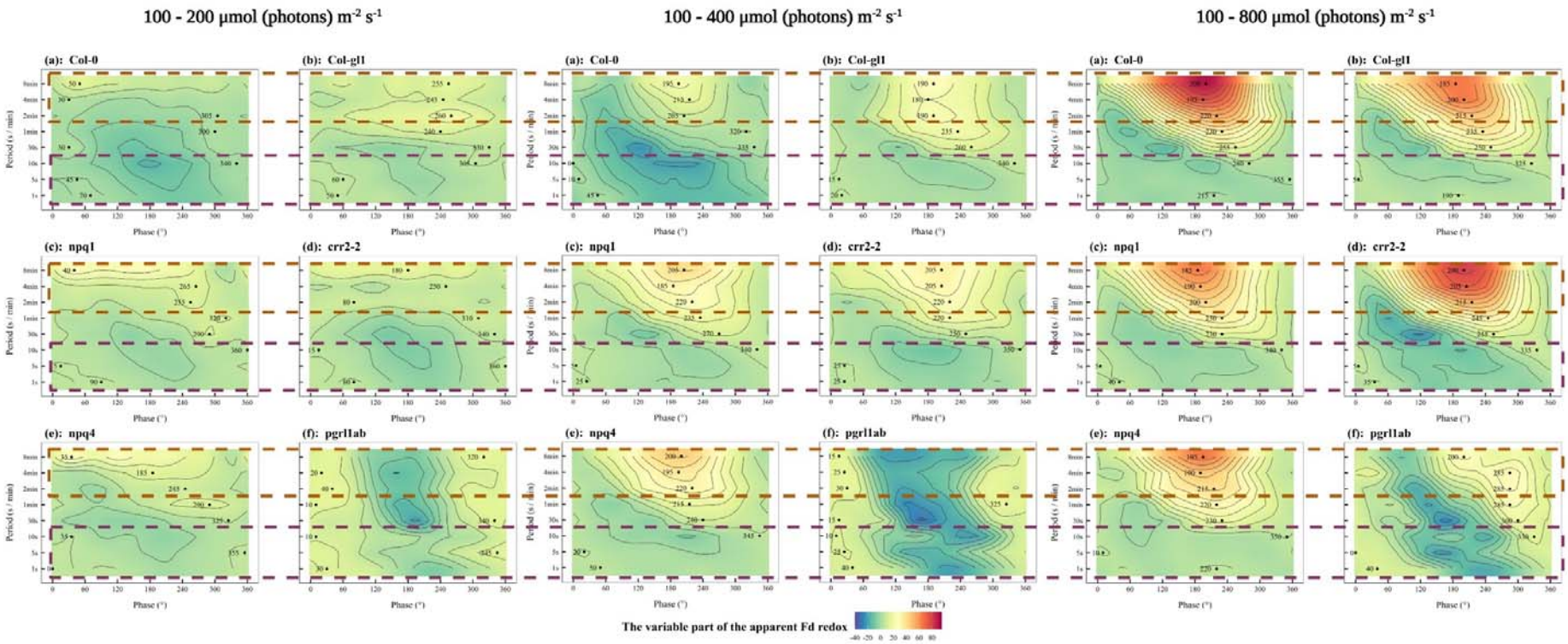

Fig.SM-5. The variable part of apparent relative Fd reduction induced in 6 genotypes of *A. thaliana* (n=3) by three different amplitudes of oscillating light. The structure of the graph and the legends are the same as in Fig.SM-1, only the color scale from blue to red to represents the apparent change of Fd redox state: Blue means more reduced than at the light minimum and red more oxidized that at the light minimum.

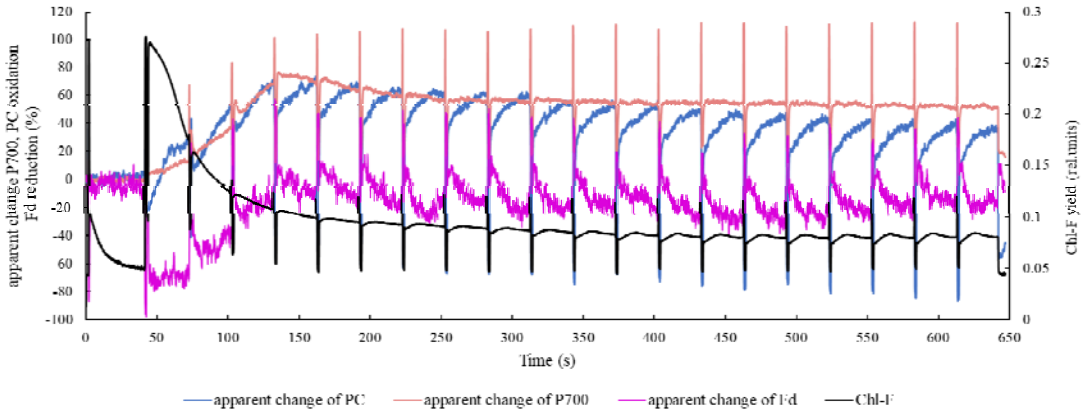

Fig.SM-6. Raw data measured with WT Col-0 show induction of chlorophyll fluorescence and apparent PC, P700 and Fd oxidation/reduction during 10-minutes of exposure to constant light. The data demonstrate convergence to a steady-state that was reached before the oscillatory light was applied.